

The Observed Growth of Massive Galaxy Clusters IV: Robust Constraints on Neutrino Properties

A. Mantz,^{1,2*} S. W. Allen² and D. Rapetti²

¹*NASA Goddard Space Flight Center, Code 662, Greenbelt, MD 20771, USA*

²*Kawli Institute for Particle Astrophysics and Cosmology at Stanford University, 452 Lomita Mall, Stanford, CA 94305-4085, USA and SLAC National Accelerator Laboratory, 2575 Sand Hill Road, Menlo Park, CA 94025, USA.*

7 April 2010

ABSTRACT

This is the fourth of a series of papers in which we derive simultaneous constraints on cosmological parameters and X-ray scaling relations using observations of the growth of massive, X-ray flux-selected galaxy clusters. Our data set consists of 238 clusters drawn from the *ROSAT* All-Sky Survey, and incorporates extensive follow-up observations using the *Chandra* X-ray Observatory. Here we examine the constraints on neutrino properties that are enabled by the precise and robust constraint on the amplitude of the matter power spectrum at low redshift available from our data. In combination with cluster gas mass fraction, cosmic microwave background, supernova and baryon acoustic oscillation data, and incorporating conservative allowances for systematic uncertainties, we limit the species-summed neutrino mass, M_ν , to < 0.33 eV at 95.4 per cent confidence in a spatially flat, cosmological constant (Λ CDM) model. In a flat Λ CDM model where the effective number of neutrino species, N_{eff} , is allowed to vary, we find $N_{\text{eff}} = 3.4^{+0.6}_{-0.5}$ (68.3 per cent confidence, incorporating a direct constraint on the Hubble parameter from Cepheid and supernova data). We also obtain results with additional degrees of freedom in the cosmological model, in the form of global spatial curvature (Ω_k) and a primordial spectrum of tensor perturbations (r and n_t). The results are not immune to these generalizations; however, in the most general case we consider, in which M_ν , N_{eff} , curvature and tensors are all free, we still obtain $M_\nu < 0.70$ eV and $N_{\text{eff}} = 3.7 \pm 0.7$ (at respectively the same confidence levels as above). These results agree well with recent work using independent data, and highlight the importance of measuring cosmic structure and expansion at low as well as high ($z \sim 1100$) redshifts. Although our cluster data extend to redshift $z = 0.5$, the direct effect of neutrino mass on the growth of structure at late times is not yet detected at a significant level.

Key words: cosmology: observations – cosmological parameters – large-scale structure of Universe – X-rays: galaxies: clusters.

1 INTRODUCTION

Observations of neutrino flavor oscillation have conclusively shown that the neutrino mass eigenstates are non-degenerate (e.g. Fukuda et al. 1998, 2002; Ahmad et al. 2002; Ahn et al. 2003, 2006; Eguchi et al. 2003; Sanchez et al. 2003; Giacomelli & Margiotta 2004; Aharmim et al. 2005). Although, these observations can place tight constraints on the differences in squared mass, measuring the absolute mass scale remains challenging. Current laboratory efforts focus on tritium beta decay (e.g. Lobashev 2003; Kraus et al. 2005) and neu-

trinoless double beta decay (e.g. Aalseth et al. 1999; Klapdor-Kleingrothaus et al. 2001; Arnaboldi et al. 2005; Arnold et al. 2005); the latter, if observed, would additionally indicate that neutrinos are Majorana rather than Dirac fermions. The squared mass differences measured from flavor oscillations place a lower bound on the sum of the three masses, $M_\nu = \sum_i m_i$, at ~ 0.056 (0.095) eV/ c^2 in the normal (inverted) hierarchy, while current tritium beta decay results provide an upper bound on the mass of the electron neutrino at ~ 2 eV/ c^2 (thus on M_ν at ~ 6 eV/ c^2).¹

Because neutrinos play a prominent role in the early

* E-mail: adam.b.mantz@nasa.gov

¹ Henceforth, we set $c = 1$.

Universe, cosmological observations are also sensitive to their properties (for a review, see Lesgourgues & Pastor 2006; see also Section 2). The primary effect of non-zero neutrino mass on cosmological observables is to suppress the formation of cosmic structure on intermediate and small scales. Comparison of the Cosmic Microwave Background (CMB), which reflects large-scale structure at early times, with measurements of the intermediate- or small-scale structure in the local Universe thus provides a way to constrain the absolute mass scale of the neutrino (e.g. Fukugita et al. 2000).

This approach has the disadvantage that any neutrino properties inferred are at some level sensitive to our incomplete understanding of cosmology, in particular dark energy and inflation. It has long been recognized, however, that using complementary measurements of structure, as described above, significantly reduces the sensitivity of the results to such necessary assumptions (e.g. Allen et al. 2003; Tegmark et al. 2004). Nevertheless, it is imperative that any systematic uncertainties affecting the measurements of cosmic structure be properly accounted for in order to obtain robust results.

The amount of structure in the local Universe is generally described by the parameter σ_8 , defined as the present day root-mean-square fluctuation of the linearly evolved matter density field, smoothed by a spherical top-hat window of comoving radius $8h^{-1}$ Mpc; here $h = H_0/100 \text{ km s}^{-1} \text{ Mpc}^{-1}$ is the normalized Hubble parameter. At present, the most robust observation for measuring this quantity is arguably the abundance of massive galaxy clusters;² recent advances in cluster simulation (e.g. Nagai et al. 2007), comparisons of different mass measurement techniques (e.g. Bradač et al. 2008; Mahdavi et al. 2008; Newman et al. 2009), and the availability of robust mass proxies (e.g. Allen et al. 2004, 2008; Kravtsov et al. 2006) have significantly reduced systematic uncertainties associated with the measurement of cluster masses. Consequently, recent estimates of σ_8 based on independent analyses of galaxy cluster data (both optically and X-ray selected clusters) are in very good agreement [$\sigma_8 \sim 0.8$; Mantz et al. 2008, 2009a (hereafter Paper I); Henry et al. 2009; Rozo et al. 2010; Vikhlinin et al. 2009]. Recent analyses of cosmic shear data are also in good agreement (Benjamin et al. 2007; Fu et al. 2008), and provide compatible constraints on the neutrino mass to our own (Tereno et al. 2009). Galaxy redshift surveys have also produced comparable results (Thomas et al. 2009).

The number of neutrino species participating in weak interactions is known to be three to high precision (Amsler et al. 2008). However, the possibility remains that additional “sterile” species exist. Results consistent with the existence of a fourth neutrino were reported by the Liquid Scintillator Neutrino Detector (LSND; Aguilar et al. 2001); these results are disfavored by the MiniBooNE experiment (Aguilar-Arevalo et al. 2009a,b), although the interpreta-

tion remains somewhat ambiguous at present. This is another question that cosmological observations can address. In particular, the synthesis of light elements is sensitive to the number of relativistic species present in the early Universe, since these determine the expansion rate at that time; however, observation of primordial deuterium and helium abundances are challenging and are subject to large systematic uncertainties. An independent probe is provided by the CMB, in combination with other cosmological data, as described in Section 2. In this work, we consider only the case where the neutrino species (whatever their number) have approximately degenerate mass; in this case, M_ν and the effective number of neutrino species, N_{eff} , are sufficient to describe the cosmological effect of neutrinos. More general mass splittings, and in particular the case favored by the initial LSND results, in which a sterile neutrino is significantly more massive than the other species, require a more complete treatment (as in, e.g., Crotty et al. 2004).

In this paper, we apply the statistically rigorous analysis method of Paper I and the X-ray flux-limited cluster samples and follow-up observations described in Mantz et al. (2009b, hereafter Paper II) to the problem of inferring neutrino properties from cosmological data. These data (collectively referred to here as the cluster X-ray Luminosity Function, or XLF) provide a robust means to measure σ_8 ; our analysis method includes generous systematic allowances and accounts fully for all parameter degeneracies. In obtaining our results, we also incorporate CMB data and measurements of cosmic distance in the form of cluster gas mass fractions (f_{gas}), type Ia supernova (SNIa) fluxes and Baryon Acoustic Oscillation (BAO) data (see Section 3 and references therein). We note that Reid et al. (2009) obtain very similar results to our own by importance sampling 5-year *Wilkinson Microwave Anisotropy Probe* (WMAP) results using a prior based on the analysis of optically selected clusters by Rozo et al. (2010).

The basic cosmology that we consider in this paper is the spatially flat, cosmological constant (Λ CDM) model parametrized by the mean baryon density, Ω_b ; the mean total matter density including baryons, neutrinos and cold dark matter (CDM), Ω_m ; the Hubble parameter, H_0 ; the normalization of the matter power spectrum, σ_8 ; the spectral index of the primordial scalar power spectrum, n_s ; and the optical depth to reionization, τ . Here the mean densities refer to the present day (redshift $z = 0$), since their values at other times are then determined by the Friedmann equation, and σ_8^2 is the $z = 0$ variance in the matter density field at scales of $8h^{-1}$ Mpc, as defined above. This simple and commonly used model assumes $M_\nu = 0$ and $N_{\text{eff}} = 3.046$, the predicted value for the three weakly interacting neutrinos.

In addition to freeing M_ν and N_{eff} , we will consider the effect of marginalizing over other parameters with which they are degenerate. However, since the flat Λ CDM model is known to provide a good fit to currently available cosmological data, we are conservative in incorporating these additional degrees of freedom. In particular, we consider generalizing the description of dark energy, either by allowing global spatial curvature or by varying the dark energy equation of state in a flat universe, and including the effects of primordial tensor perturbations. The former case is parameterized by the effective curvature energy density, Ω_k , or the equation of state parameter, w , while in the latter case we

² We note that current cluster measurements do not constrain σ_8 independent of spectral index of the power spectrum, n_s . However, the best fitting value of σ_8 does not vary rapidly with n_s ; moreover, n_s is well constrained by CMB data in all cosmological models considered here.

simultaneously marginalize over the tensor-to-scalar ratio, r (defined with respect to wavenumber $k = 0.002h \text{ Mpc}^{-1}$, as in, e.g., Komatsu et al. 2009), and the tensor power spectral index, n_t .

In our results, we will consistently quote one-sided limits (upper bounds) on M_ν and r at the 95.4 per cent confidence level and two-sided constraints on all other parameters at 68.3 per cent confidence.

2 BACKGROUND

Although the purpose of this work is to explore the constraints enabled by the XLF data, it is instructive to begin by considering the cosmological constraints on M_ν that have been obtained without using measurements of local cosmic structure. As described by Ichikawa et al. (2005), Dunkley et al. (2009) and Komatsu et al. (2009), CMB observations alone provide a limit that, while weak ($M_\nu < 1.3 \text{ eV}$ at 95.4 per cent confidence), is relatively robust to assumptions about dark energy and primordial tensors.³ While we do not review the details here, the constraint arises because the effect of neutrino mass on the CMB temperature anisotropy spectrum is qualitatively different when neutrinos are relativistic compared with non-relativistic during the decoupling epoch. In particular, for $M_\nu < 1.5 \text{ eV}$, changes in M_ν can be easily mimicked by a corresponding change in the Hubble parameter, H_0 . As a result, M_ν is strongly degenerate with H_0 in analyses using only CMB data, which does not itself constrain H_0 . The combination of CMB data with distance measurements in the form of SNIa and BAO data can place a constraint on H_0 , improving the limits on M_ν by roughly a factor of two ($M_\nu < 0.67 \text{ eV}$ for a spatially flat ΛCDM background; Komatsu et al. 2009).

As we will show, the inclusion of a measurement of local cosmic structure in the form of galaxy cluster abundance can improve these limits by another factor of two or greater, and furthermore greatly increase the robustness of the results to assumptions about the nature of dark energy and inflation. This improvement is possible because the combination of large-scale, high-redshift and intermediate-scale, low-redshift measurements of cosmic structure exploits the defining characteristic of light, weakly interacting particles: they are relativistic during the earliest stages of cosmic structure formation but non-relativistic at the present day.⁴ The imprint of neutrinos on cosmic structure, and in particular on the growth of structure from the surface of last scattering to the present, thus differs from that of the photon background (relativistic at all times) and CDM (assumed to be non-relativistic at all times). In particular, a non-zero mass in neutrinos results in a net suppression of the growth of structure on scales smaller than their free-streaming length

(approximately corresponding to wavenumber $10^{-2}h \text{ Mpc}^{-1}$ today) relative to an equal mass in CDM (Bond et al. 1980).

In practical terms, the constraint on M_ν arising from the combination of CMB and cluster data can be understood as follows. Even when $M_\nu \neq 0$, the CMB data provide a good constraint on the high-redshift amplitude of the power spectrum, since the direct effect of neutrino mass on the observed temperature anisotropies is relatively small. However, the late-time, intermediate-scale power spectrum amplitude (the value of σ_8) that would be predicted based on that high-redshift constraint is very sensitive to M_ν , since neutrino mass suppresses the development of structure on those scales. This strong degeneracy is apparent in the blue confidence regions in Figure 1. By constraining σ_8 independent of M_ν , clusters (or other low-redshift structure measurements) break this degeneracy, improving the constraints on neutrino mass (gold contours in the figure).

Even more power is available if the growth of structure can be measured, exploiting the time-dependent nature of the effects of neutrino mass on cosmic structure development (e.g. Lesgourgues & Pastor 2006). However, we show in Section 5.1 that the growth of structure in current cluster data, while able to constrain models of dark energy (Paper I; Vikhlinin et al. 2009) and modified gravity (Rapetti et al. 2009a,b; Schmidt et al. 2009), are not yet sufficient to contribute to constraints on M_ν .

In the case of the effective number of relativistic species, N_{eff} , CMB data alone can provide a lower bound, due to the gravitational effect of their anisotropic stress. Apart from providing this bound, however, the CMB data are hampered by a near-perfect degeneracy between N_{eff} and $\Omega_m h^2$, the physical matter density (Dunkley et al. 2009). This degeneracy arises because CMB observations do not constrain either N_{eff} or $\Omega_m h^2$ directly, only the redshift of matter-radiation equality, z_{eq} , which is a function of both parameters. Again, the addition of cosmic distance measurements can reduce the effect of this degeneracy by placing an independent constraint on $\Omega_m h^2$; Komatsu et al. (2009) obtained $N_{\text{eff}} = 4.4 \pm 1.5$ (68 per cent confidence).

Measurements of local structure can also contribute to improved constraints on N_{eff} , as we show in Section 6. The contribution of clusters to this problem is less direct than in the case of M_ν : the constraint on σ_8 and Ω_m from cluster data improves the constraint on $\Omega_m h^2$ from the CMB+distance measurements (e.g. Figure 1 of Paper I), indirectly improving the constraint on N_{eff} through the degeneracy described above.

3 DATA

The galaxy cluster data used in this work, as well as their selection and reduction, are discussed in detail in Paper II. Using three wide-area cluster samples drawn from the *ROSAT* All-Sky Survey (RASS; Trümper 1993) – the *ROSAT* Brightest Cluster Sample (BCS; Ebeling et al. 1998), the *ROSAT*-ESO Flux-Limited X-ray sample (REFLEX; Böhringer et al. 2004), and the bright sub-sample of the Massive Cluster Survey (Bright MACS; Ebeling et al. 2001, 2010) – we select a statistically complete sample of 238 X-ray luminous clusters covering the redshift range $z < 0.5$. Of these 238 clusters, 94 have follow-up *Chan-*

³ We note that this constraint is not entirely robust, and can be significantly degraded when multiple additional degrees of freedom are included in the cosmological model. In several of the models we consider, the combination of CMB data and cosmic distance measurements produces weaker constraints; however, in the worst case, the upper limit is still $\sim 2.5 \text{ eV}$ (Tables 1 and 2).

⁴ The latter condition follows from the lower bound $M_\nu > 0.056 \text{ eV}$ obtained from flavor oscillation measurements.

dra or *ROSAT* observations that we incorporate into the analysis. From the follow-up observations, we measure X-ray luminosity, average temperature, and gas mass within r_{500} .⁵ The gas mass is used as a proxy for total mass, using the finding of Allen et al. (2008) that the gas mass fraction, $f_{\text{gas}} = M_{\text{gas}}/M_{\text{tot}}$, is a constant for hot, massive clusters (see also Section 4). Cluster f_{gas} measurements additionally provide a precise measure of cosmic distance, so we include the full data set and analysis of Allen et al. in this work.

In addition to these cluster data sets, we incorporate CMB, SNIa and BAO data. Our analysis of the CMB anisotropies uses 5-year *WMAP* data (Hinshaw et al. 2009; Hill et al. 2009; Nolta et al. 2009) with the March 2008 version of the *WMAP* likelihood code⁶ (Dunkley et al. 2009), as well as Arcminute Cosmology Bolometer Array Receiver (ACBAR) data at smaller angular scales (Reichardt et al. 2009) and measurements of the CMB polarization from the Background Imaging of Cosmic Extragalactic Polarization (BICEP) instrument (Chiang et al. 2009). The SNIa results are derived from the Union compilation (Kowalski et al. 2008), which includes data from a variety of sources (307 SNIa in total; see references in Paper I). Our analysis of BAO data uses the constraints on the ratio of the sound horizon to the distance scale at $z = 0.25$ and $z = 0.35$ derived by Percival et al. (2007) from the galaxy correlation function in 2dF (Colless et al. 2001, 2003) and Sloan Digital Sky Survey (Adelman-McCarthy et al. 2007) data. Finally, we employ in some cases a Gaussian prior on the Hubble parameter, $h = 0.742 \pm 0.036$, based on the results of Riess et al. (2009).⁷

4 ANALYSIS METHOD AND SYSTEMATICS

Our results are obtained via Markov Chain Monte Carlo (MCMC), employing the Metropolis sampler embedded in the COSMOMC code of Lewis & Bridle (2002).⁸ The May 2008 COSMOMC release includes the 5-year *WMAP* and Union supernova data and analysis codes; an additional module implementing the f_{gas} analysis has also been publicly released (Rapetti et al. 2005; Allen et al. 2008).⁹ Further modifications were made to include the likelihood codes for the XLF and BAO data. The CMB and matter power spectrum calculations were performed using the CAMB package of Lewis, Challinor, & Lasenby (2000).¹⁰

When analyzing the CMB data, we marginalize over a plausible range in the amplitude of the Sunyaev-Zel'dovich signal due to galaxy clusters ($0 < A_{\text{SZ}} < 2$; introduced by Spergel et al. 2007). Our analysis of the Union supernova sample of Kowalski et al. (2008) includes their treatment of

systematic uncertainties, which accounts for the effects of Malmquist bias and uncertainties in lightcurve fitting and photometry (among others).

The method used to analyze cluster f_{gas} data is described in full by Allen et al. (2008). It incorporates generous systematic allowances for instrument calibration (10 per cent), non-thermal pressure support (10 per cent, Nagai et al. 2007), the depletion of baryons in clusters with respect to the cosmic mean (20 per cent), and evolution with redshift of the baryonic and stellar content of clusters (10 and 20 per cent).

The analysis of the XLF data is detailed in Paper I. The method combines cluster survey data with follow-up observations in an internally consistent way, rigorously accounting for the effects of Malmquist and Eddington biases and parameter degeneracies. Conservative systematic allowances are included to account for uncertainty in the predicted cluster mass function, the overall cluster survey completeness and purity, and instrument calibration.

As discussed in Section 2 and illustrated in Sections 5 and 6, the XLF data contribute to constraints on M_ν and N_{eff} through their measurement of σ_8 . The posterior uncertainty on this measurement (from the XLF alone) is ~ 6 per cent, and is dominated by systematic uncertainty, as described in Paper I. Specifically, the uncertainty in σ_8 is determined by the accuracy with which cluster masses can be measured. As detailed in Paper II, we do not directly infer cluster masses at r_{500} by assuming hydrostatic equilibrium of the intracluster medium, a procedure which, when applied to a typical cluster, introduces a large and highly variable bias (Faltenbacher et al. 2005; Rasia et al. 2006; Nagai et al. 2007). Instead, we use the gas mass at r_{500} , which can be measured without significant bias, as a proxy for total mass. The proxy relation is calibrated using the f_{gas} data of Allen et al. (2008), which effectively consist of gas mass and total mass measurements for the subset of clusters where the hydrostatic assumption is applicable (the most massive, dynamically relaxed clusters). Of the systematic allowances described above, the most relevant for this procedure are the allowances for non-thermal support and instrument calibration in the f_{gas} analysis. In addition, we account for uncertainty in the difference in f_{gas} between r_{2500} (as measured by Allen et al.) and r_{500} , as well as possible scatter in f_{gas} from cluster to cluster (see Paper II). Ultimately, both our estimates of individual masses and the mean cluster mass scale include a systematic error budget of ~ 15 per cent.

5 LIMITS ON M_ν

5.1 Simple models

We first consider the case of a spatially flat Λ CDM cosmology with non-zero neutrino mass. For this model, the joint 68.3 and 95.4 per cent confidence regions in the M_ν - σ_8 plane from the combination of CMB, f_{gas} , SNIa and BAO data appear in the left panel of Figure 1 (blue contours). The 95.4 per cent confidence upper bound on M_ν from these data (including the systematic allowances described in Section 4) is $M_\nu < 0.61$ eV (Table 1), a marginal improvement over that obtained by Komatsu et al. (2009) using only *WMAP*, SNIa and BAO data.

⁵ r_{500} is defined to be the radius within which the mean enclosed density is 500 times the critical density at the cluster's redshift.

⁶ <http://lambda.gsfc.nasa.gov>

⁷ Strictly speaking, this result should be interpreted as a constraint on the luminosity distance to $z \sim 0.04$, as noted by Reid et al. (2009). However, as those authors conclude, the distinction between that approach and a straightforward prior on h is very small in practice.

⁸ <http://cosmologist.info/cosmomc/>

⁹ http://www.stanford.edu/~drapetti/fgas_module/

¹⁰ <http://www.camb.info>

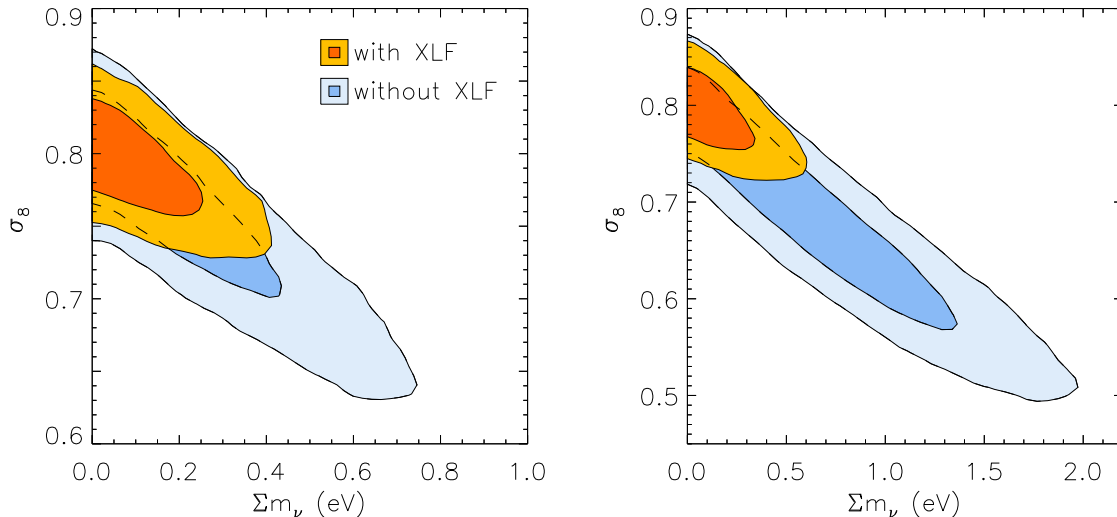


Figure 1. Joint 68.3 and 95.4 per cent confidence regions in the M_ν - σ_8 plane from the combination of CMB, f_{gas} , SNIa and BAO data (blue), and the combination of those data with the XLF (gold). The XLF data provide a tight constraint on σ_8 , breaking the degeneracy in this plane. To demonstrate the robustness of constraints on M_ν obtained using the XLF data, we compare (left panel) results for a simple Λ CDM+ M_ν model with (right panel) results obtained when nuisance parameters are included in the model (in this case, Ω_k , r and n_t ; note the difference in scale). Note that conservative systematic uncertainties are included here (and in all subsequent figures).

However, it is clear in the figure that a tight constraint on σ_8 can improve the limits on M_ν . The upper limit obtained by including the XLF data, which provide such a constraint, is $M_\nu < 0.33$ eV (corresponding to the gold contours in Figure 1), nearly a factor of two improvement.

We note that when the results excluding the XLF data are combined with the Gaussian prior $\sigma_8 = 0.82 \pm 0.05$, based on the XLF results for a flat Λ CDM cosmology with $n_s = 0.95$ (Paper I), the limits on M_ν obtained are virtually identical to those from the full combination of data, $M_\nu < 0.33$ eV. From this we conclude that the XLF data currently contribute to the bound on M_ν only through their ability to constrain σ_8 ; the effect of non-zero neutrino mass on the (time-dependent) growth of structure is not detected in the present data.

5.2 Extended models

Next, we consider how the neutrino mass limits are affected when additional degrees of freedom are introduced in the cosmological model. Several possibilities are worth considering here. To begin with, the model for dark energy may be generalized; the simplest ways to accomplish this by introducing a single additional free parameter are through the spatial curvature (i.e. by not linking the dark energy density directly to the matter density) and through the equation of state, retaining the assumption of spatial flatness in the latter case. The flat Λ CDM case corresponds to effective curvature density $\Omega_k = 0$ and equation of state $w = -1$. Since current data do not support departures from the flat Λ CDM model either through $\Omega_k \neq 0$ or $w \neq -1$, we consider these cases separately rather than introducing both parameters simultaneously. Secondly, we consider the effect of primordial tensor modes, parametrized through the tensor-to-scalar ratio, r . We additionally marginalize over the tensor spectral index, n_t , rather than assuming a particular model of inflation where n_t would be linked to r via a consistency relation.

Finally, we consider the effect of varying N_{eff} on the bounds obtained for M_ν , leaving a discussion of the constraints on N_{eff} itself for Section 6.

The effects of adding each of these degrees of freedom individually to the Λ CDM+ M_ν model are displayed in Figure 2 (95.4 per cent confidence regions only). The left panel shows results from the combination of CMB, SNIa, BAO and f_{gas} data. Here it is clear that degeneracies exist between M_ν and some of the additional parameters. In particular, the presence of primordial tensor modes ($M_\nu < 0.92$ eV) or curvature ($M_\nu < 1.44$ eV) significantly degrades the limits on neutrino mass relative to the simpler model ($M_\nu < 0.61$ eV) by lengthening the major axis of the confidence region. In contrast, while N_{eff} has a small effect on the M_ν limit ($M_\nu < 0.67$ eV), it significantly degrades the constraints on other cosmological parameters, including σ_8 , resulting in the much thicker confidence region in the figure (see also Section 6.1). The equation of state of dark energy is an intermediate case which increases the bound on the neutrino mass somewhat ($M_\nu < 0.75$ eV), while also degrading the constraints on other parameters slightly. Marginalized confidence intervals on parameters of interest for these cases can be found in Table 1.

The right panel of Figure 2 shows the equivalent tests when the XLF data are included in the analysis. In this case, the weakest constraint occurs when N_{eff} is free ($M_\nu < 0.54$ eV); this is sensible, since it had the smallest correlation with σ_8 a priori (left panel). In the other cases shown, limits on M_ν are improved by a factor of 2–3. In the most general model considered, where curvature, tensors and additional relativistic species are all marginalized over, the full combination of data yields $M_\nu < 1.31$ eV, compared with $M_\nu < 2.34$ eV when the XLF is not used (Table 1).

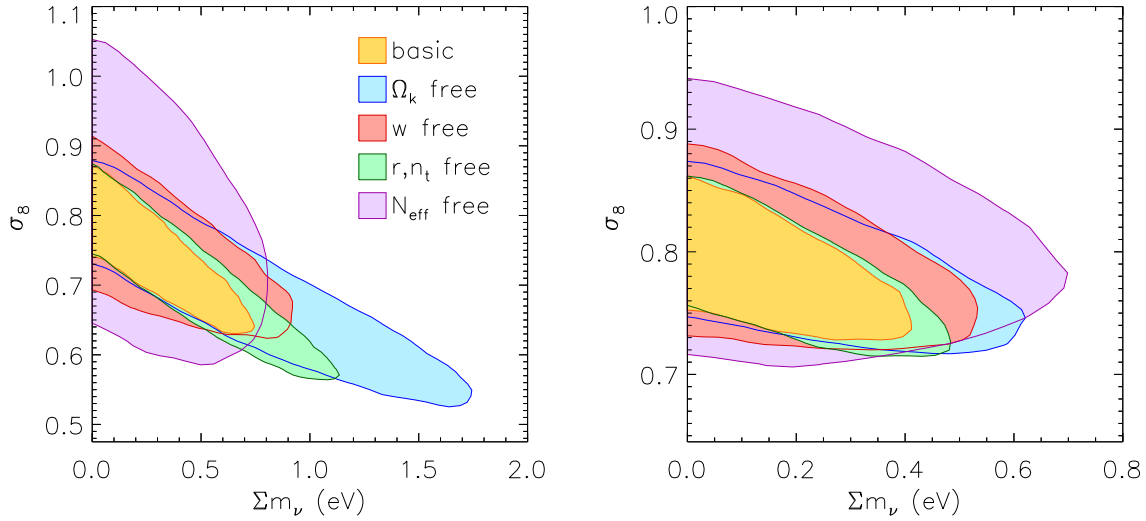


Figure 2. [preprint note: a monochrome version of this figure appears after the references, as Figure 6] Joint 95.4 per cent confidence regions for M_ν and σ_8 for various cosmological models. Yellow contours correspond to the basic Λ CDM+ M_ν model, blue contours are marginalized over Ω_k , red contours over w , green over r and n_t , and purple over N_{eff} . The left panel shows constraints obtained from the combination of CMB, f_{gas} , SNIa and BAO data; the right panel shows results that include the XLF in addition to those data. No external prior on H_0 is used.

Table 1. Constraints on the species-summed neutrino mass and other model parameters, including conservative systematic allowances. Note that limits on M_ν and r are listed at 95.4 per cent confidence, while all others are 68.3 per cent confidence. Parameters with a single value listed were fixed at that value. Constraints on Ω_m do not appear in the table, as they were extremely similar for all models, consistent with $\Omega_m = 0.26 \pm 0.015$. The first column indicates whether the XLF data were included in the fit; the combination of CMB, f_{gas} , SNIa and BAO data is used in all cases. The results in this table do not use an external prior on H_0 . The use of such a prior, in addition to the XLF data, greatly improves constraints on both N_{eff} and M_ν when N_{eff} is a free parameter (see Table 2).

XLF	σ_8	Ω_k	w	r	n_t	N_{eff}	M_ν (eV)
	0.77 ± 0.05	0	-1	0	0	3.046	< 0.61
✓	0.79 ± 0.03	0	-1	0	0	3.046	< 0.33
	0.72 ± 0.08	0.009 ± 0.008	-1	0	0	3.046	< 1.44
✓	0.79 ± 0.03	0.004 ± 0.006	-1	0	0	3.046	< 0.50
	0.76 ± 0.05	0	-1.02 ± 0.08	0	0	3.046	< 0.72
✓	0.79 ± 0.03	0	-1.03 ± 0.07	0	0	3.046	< 0.43
	0.76 ± 0.06	0	-1	< 0.33	$0.3^{+0.8}_{-0.7}$	3.046	< 0.92
✓	0.79 ± 0.03	0	-1	< 0.22	$0.5^{+0.7}_{-0.8}$	3.046	< 0.38
	0.80 ± 0.09	0	-1	0	0	$3.4^{+2.0}_{-1.3}$	< 0.67
✓	0.80 ± 0.04	0	-1	0	0	$3.6^{+1.4}_{-1.0}$	< 0.54
	0.69 ± 0.08	0.008 ± 0.009	-1	< 0.29	$0.5^{+0.8}_{-0.8}$	3.046	< 1.60
✓	0.79 ± 0.03	0.003 ± 0.006	-1	< 0.19	$0.1^{+0.8}_{-0.8}$	3.046	< 0.49
	0.72 ± 0.10	0.010 ± 0.009	-1	0	0	$3.4^{+2.0}_{-1.2}$	< 1.84
✓	0.79 ± 0.04	0.007 ± 0.007	-1	0	0	$3.6^{+1.7}_{-0.9}$	< 1.14
	0.79 ± 0.10	0	-1	< 0.43	$0.2^{+0.6}_{-0.7}$	$4.5^{+2.2}_{-2.0}$	< 1.46
✓	0.81 ± 0.05	0	-1	< 0.33	$0.2^{+0.7}_{-0.8}$	$4.5^{+1.4}_{-1.6}$	< 0.95
	0.71 ± 0.10	0.008 ± 0.009	-1	< 0.36	$0.4^{+0.6}_{-0.7}$	$4.5^{+2.2}_{-2.1}$	< 2.34
✓	0.80 ± 0.04	0.004 ± 0.008	-1	< 0.30	$0.1^{+0.8}_{-0.7}$	$4.0^{+1.9}_{-1.1}$	< 1.31

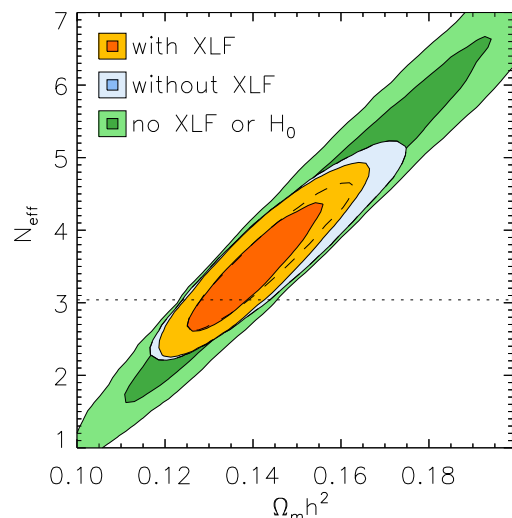


Figure 3. Joint 68.3 and 95.4 per cent confidence regions on $\Omega_m h^2$ and N_{eff} from the combination of CMB, f_{gas} , SNIa and BAO data with a direct measurement of H_0 (blue), and the same data with the addition of the XLF (gold). Also shown are the constraints from the former combination of data, but without the prior on H_0 (green); this illustrates the strong sensitivity of the N_{eff} results to the Hubble parameter. The dotted, horizontal line indicates the standard value of N_{eff} , 3.046.

6 CONSTRAINTS ON N_{eff}

6.1 Simple models

Joint constraints on N_{eff} and $\Omega_m h^2$ are shown in Figure 3 for a flat Λ CDM cosmology. The strong correlation in this plane is due to the fact that the CMB data constrain directly z_{eq} , which is a degenerate combination of N_{eff} and $\Omega_m h^2$, as discussed previously in Section 2. The combination of data that we use places tight constraints on Ω_m , so significant improvement can be obtained by incorporating a direct measurement of the Hubble constant; throughout this section we use a Gaussian prior, $h = 0.742 \pm 0.036$, based on the results of Riess et al. (2009). The constraints thus obtained are listed in Table 2.

We note that, ordinarily, the combination of f_{gas} and CMB data provides a tight constraint on H_0 (Allen et al. 2008); however, this is not the case when N_{eff} is free. The reason why can be seen in Figure 4. The green contours in the figure show constraints obtained from combining the CMB, f_{gas} , SNIa and BAO data (without a prior on H_0). A correlation in this plane occurs naturally in the f_{gas} analysis, since X-ray observations of clusters measure a degenerate combination of the cosmic baryon fraction, Ω_b/Ω_m , and distance. When N_{eff} is fixed, CMB data place tight constraints on the baryon fraction, though not on the Hubble parameter, and so the combination of CMB and f_{gas} data produces tight constraints on both H_0 and Ω_b/Ω_m . When N_{eff} is free, however, the CMB constraints in this plane are degenerate along nearly the same axis as the f_{gas} constraints,¹¹ and so the inclusion of additional, independent distance measurements is necessary to place a constraint on H_0 . The com-

¹¹ Respectively, the quantities $\Omega_m h^2$ and $\Omega_m h^{1.5}$ are degenerate in the analysis of CMB and f_{gas} data.

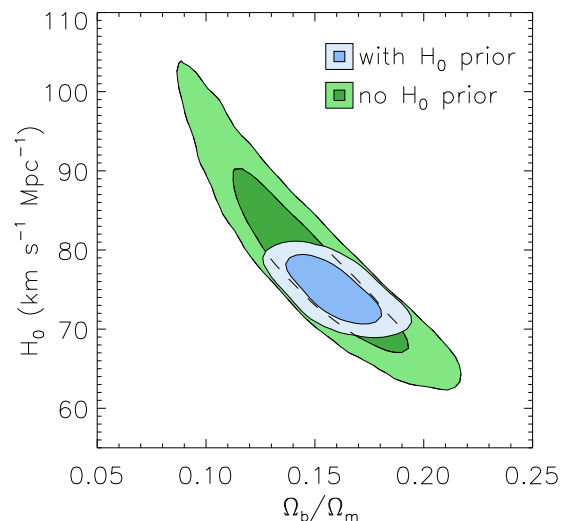


Figure 4. Joint constraints on Ω_b/Ω_m and H_0 when N_{eff} is free. Green contours show results obtained from the combination of CMB, f_{gas} , SNIa and BAO data; despite the inclusion of SNIa and BAO data, the strong degeneracy in this plane that occurs in both f_{gas} and CMB analyses (when N_{eff} is free) remains evident. The addition of a measurement of the Hubble parameter at the 5 per cent level (blue contours) significantly improves the results.

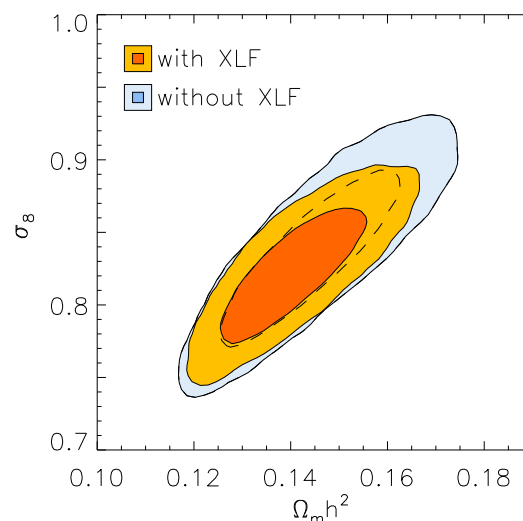


Figure 5. Joint 68.3 and 95.4 per cent confidence regions on $\Omega_m h^2$ and σ_8 from the combination of CMB, f_{gas} , SNIa and BAO data with a direct measurement of H_0 (blue), and the same data with the addition of the XLF (gold) when N_{eff} is free. The tight constraint on σ_8 provided by the XLF data improves the determination of $\Omega_m h^2$, which translates to an improved constraint on N_{eff} (Figure 3).

ination with a direct measurement of H_0 (blue contours) significantly improves matters.

As Figure 3 shows, the addition of the XLF data improves the constraint on N_{eff} somewhat, from $N_{\text{eff}} = 3.6^{+0.7}_{-0.6}$ to $N_{\text{eff}} = 3.4^{+0.6}_{-0.5}$ (68.3 per cent confidence). The mechanism for this improvement is a degeneracy between $\Omega_m h^2$ and σ_8 , shown in Figure 5, which the XLF data reduce through their constraint on σ_8 .

Table 2. Constraints on the neutrino effective number and other model parameters. Note that limits on M_ν and r are listed at 95.4 per cent confidence, while all others are 68.3 per cent confidence. Parameters with a single value listed were fixed at that value. The first two columns respectively indicate whether the prior on H_0 and the XLF data were included in the fit; the combination of CMB, f_{gas} , SNIa and BAO data is used in all cases.

H_0	XLF	σ_8	Ω_k	r	n_t	N_{eff}	M_ν (eV)
		0.86 ± 0.07	0	0	0	$3.8^{+1.9}_{-1.5}$	0
✓		0.83 ± 0.04	0	0	0	$3.6^{+0.7}_{-0.6}$	0
✓	✓	0.82 ± 0.03	0	0	0	$3.4^{+0.6}_{-0.5}$	0
		0.85 ± 0.07	0.002 ± 0.006	0	0	$3.4^{+1.8}_{-1.3}$	0
✓		0.83 ± 0.04	0.001 ± 0.005	0	0	$3.4^{+0.8}_{-0.7}$	0
		0.88 ± 0.08	0	< 0.25	$0.1^{+0.9}_{-0.7}$	$4.2^{+2.6}_{-1.7}$	0
✓		0.83 ± 0.04	0	< 0.20	$0.3^{+0.9}_{-0.9}$	$3.6^{+0.7}_{-0.8}$	0
		0.80 ± 0.09	0	0	0	$3.4^{+2.0}_{-1.3}$	< 0.67
✓		0.79 ± 0.05	0	0	0	$3.5^{+0.9}_{-0.4}$	< 0.64
✓	✓	0.80 ± 0.03	0	0	0	$3.5^{+0.7}_{-0.5}$	< 0.48
		0.72 ± 0.10	0.010 ± 0.009	0	0	$3.4^{+2.0}_{-1.2}$	< 1.84
✓		0.73 ± 0.08	0.008 ± 0.009	0	0	$3.4^{+0.9}_{-0.6}$	< 1.58
✓	✓	0.79 ± 0.03	0.005 ± 0.006	0	0	$3.5^{+0.8}_{-0.5}$	< 0.72
		0.79 ± 0.10	0	< 0.43	$0.2^{+0.6}_{-0.7}$	$4.5^{+2.2}_{-2.0}$	< 1.46
✓		0.76 ± 0.07	0	< 0.34	$0.2^{+0.7}_{-0.7}$	$3.7^{+0.7}_{-0.9}$	< 1.14
✓	✓	0.80 ± 0.04	0	< 0.23	$0.3^{+0.9}_{-0.8}$	$3.6^{+0.8}_{-0.6}$	< 0.55
		0.71 ± 0.10	0.008 ± 0.009	< 0.36	$0.4^{+0.6}_{-0.7}$	$4.5^{+2.2}_{-2.1}$	< 2.34
✓		0.71 ± 0.09	0.006 ± 0.009	< 0.33	$0.4^{+0.7}_{-0.7}$	$3.7^{+0.7}_{-0.8}$	< 1.75
✓	✓	0.80 ± 0.04	0.002 ± 0.007	< 0.29	$0.2^{+0.8}_{-0.7}$	$3.7^{+0.7}_{-0.7}$	< 0.70

6.2 Extended models

The addition of nuisance parameters in the form of curvature, tensors, and non-zero neutrino mass tends to weaken the constraints on N_{eff} and H_0 along their primary degeneracy axis, similarly to what was observed in Section 5.2. Table 2 lists the constraints obtained with and without the H_0 prior when various nuisance parameters are marginalized over, as well as when the XLF data are included in the fit. As the table shows, the inclusion of the prior on H_0 effectively eliminates the degeneracies between N_{eff} and the nuisance parameters; in particular, the constraint on N_{eff} obtained when marginalizing over curvature, tensors and neutrino mass simultaneously, $N_{\text{eff}} = 3.7^{+0.7}_{-0.8}$, is very similar to those obtained when the nuisance parameters are fixed, $N_{\text{eff}} = 3.6^{+0.7}_{-0.6}$. With so much extra freedom in the model, the inclusion of the XLF data produces only a small improvement in N_{eff} in that case.

7 PROSPECTS FOR IMPROVEMENT

An interesting question is where future improvements in the determination of M_ν and N_{eff} from cosmological data will come from. One simple way of addressing this is to see what other cosmological parameters are most correlated with the parameters of interest in the current results. We consider the simple cases of a Λ CDM model where either M_ν or N_{eff} is

additionally free, as well as the more general case with both parameters free in addition to curvature and tensor modes.

7.1 Improvements on M_ν

When only M_ν is additionally free, it remains most degenerate with σ_8 , despite the tight constraints placed on this parameter by current data, with a correlation coefficient of $\rho = -0.63$. In the more general model (with M_ν , N_{eff} , Ω_k , r and n_t free), the degeneracy with σ_8 is also relatively important ($\rho = -0.51$), but degeneracies with $\Omega_m h^2$ ($\rho = 0.60$) and Ω_k ($\rho = 0.48$) appear at approximately the same level.

The situation will change, however, with the availability of improved CMB data from *Planck*, and ultimately from future high-resolution CMB polarization and lensing observations. These new data will tighten constraints on a number of parameters that contribute to the width of the degenerate region in the M_ν - σ_8 plane,¹² (Figures 1 and 2; Kaplinghat et al. 2003; Bashinsky & Seljak 2004; Colombo et al. 2009; de Putter et al. 2009) resulting in a stronger correlation of M_ν with σ_8 .

Using a simulated *Planck* data set produced using the

¹² In addition to the curvature and tensor parameters discussed in this paper, standard cosmological parameters such as $\Omega_m h^2$, τ , n_s and the high-redshift power spectrum amplitude all contribute to the width.

FUTURCMB code of Perotto et al. (2006), we project that such data, combined with a 2 per cent constraint on σ_8 , will produce a limit $M_\nu < 0.18$ eV for minimal neutrino mass in the normal hierarchy ($M_\nu = 0.056$ eV). Alternatively, $M_\nu = 0$ would be ruled out at approximately 1σ significance for minimal neutrino mass in the inverted hierarchy ($M_\nu = 0.095$ eV). A constraint on σ_8 at this level may be possible in the near term from galaxy cluster observations, primarily by better understanding cluster mass measurements (e.g. Mahdavi et al. 2008; Zhang et al. 2010; von der Linden et al., in preparation), as well as from improved measurements of the CMB power spectrum at multipoles ~ 2000 (Lueker et al. 2009; Fowler et al. 2010; Komatsu et al. 2010).

As growth of structure data become available at higher redshifts, the time-dependent effects of neutrino mass on structure formation will also provide a powerful and more direct constraint on M_ν . Future cluster surveys may provide limits an order of magnitude better than current results (Wang et al. 2005). Eventually, other cosmological observables, e.g. the cross-correlation of Lyman-alpha absorption with CMB convergence (Vallinotto et al. 2009), may extend measurements of structure formation to even higher redshifts ($z \sim 2$).

7.2 Improvements on N_{eff}

Unsurprisingly, the correlation of N_{eff} with $\Omega_m h^2$ is dominant in both the simple ($\Lambda\text{CDM}+N_{\text{eff}}$) and more general (M_ν , N_{eff} , Ω_k , r and n_t free) models, respectively with $\rho = 0.94$ and 0.87 , although we note that in the simple case there is also a strong degeneracy with σ_8 ($\rho = 0.73$). Thus, improved measurements of the Hubble parameter and/or mean matter density will be very significant for cosmological constraints on N_{eff} .

In particular, we consider the possibility of a direct constraint on H_0 at the 2 per cent level. Such a constraint could come from several avenues, including *Spitzer* (and ultimately the *James Webb Space Telescope*) observations of Cepheids and SNIa (Freedman 2009; Riess et al. 2009), gravitational lensing time delays (e.g. Saha et al. 2006; Oguri 2007; Coe & Moustakas 2009; Dobke et al. 2009), or the comparison of the Compton- y parameter inferred from Sunyaev-Zel'dovich and X-ray observations of clusters (Schmidt et al. 2004; Bonamente et al. 2006; Rapetti et al. 2008). The latter two naturally complement efforts to extend measurements of the growth of structure using clusters to larger samples and higher redshifts. Even with no other improvements in cosmological data, such a measurement (we take $h = 0.72 \pm 0.0144$, for concreteness) would provide a constraint $N_{\text{eff}} = 3.04 \pm 0.35$ in the simple $\Lambda\text{CDM}+N_{\text{eff}}$ model, or $N_{\text{eff}} = 3.14 \pm 0.48$ in the general model (parameters listed above; 68.3 per cent confidence). Since N_{eff} and M_ν are degenerate in this model, the upper limit on M_ν would also be improved, from 0.70 to 0.55 eV.

8 CONCLUSION

We have applied measurements of the growth of massive galaxy clusters (detailed in Papers I and II), in combination

with other cosmological data, to the problem of constraining the species-summed neutrino mass, M_ν , and effective number, N_{eff} .

Our results show that a robust measurement of σ_8 from clusters significantly improves limits on M_ν from current data, and reduces their sensitivity to assumptions about the cosmological model. In a simple $\Lambda\text{CDM}+M_\nu$ cosmology, the addition of the XLF data improves the 95.4 per cent confidence upper limit on M_ν to 0.33 eV, compared with 0.61 eV from the combination of CMB, f_{gas} , SNIa and BAO data. In a more general model, marginalized over spatial curvature, primordial tensors and the effective number of neutrinos, and incorporating a prior on the Hubble parameter, the XLF data improve the limit from 1.75 eV to 0.7 eV. The results indicate that this improvement is due entirely to the ability of the cluster data to constrain σ_8 (at $z = 0$); while measurements of the (z -dependent) growth of structure in principle contain additional information about M_ν , current data are not sufficient to exploit it.

The cluster data additionally improve constraints on the effective number of relativistic species, from $N_{\text{eff}} = 3.6^{+0.7}_{-0.6}$ to $N_{\text{eff}} = 3.4^{+0.6}_{-0.5}$ in a simple $\Lambda\text{CDM}+N_{\text{eff}}$ model (68.3 per cent confidence). For the more general model, including curvature, tensors and neutrino mass, only a marginal improvement is observed.

The results obtained here are compatible with other recent estimates based on galaxy clusters (Reid et al. 2009; Vikhlinin et al. 2009), reflecting the good agreement in recent σ_8 constraints based on X-ray and optically selected clusters (Paper I; Henry et al. 2009; Rozo et al. 2010). Although current cosmological data are not sufficient to rule out the existence of sterile neutrino species or distinguish between the normal and inverted mass hierarchies, they continue to provide some of the tightest constraints available, in particular on the mass scale.

We also consider the prospects for further improvement, finding that a few per cent level measurement of the Hubble parameter will significantly improve the constraints on models where N_{eff} is free. A similarly improved determination of σ_8 , combined with improved CMB data from *Planck*, will further tighten limits on the neutrino mass scale,¹³ perhaps providing the first hints of non-zero mass from cosmological data. More precise measurements of the growth of structure at late times, and the extension of such data to higher redshifts, will provide a powerful, new mechanism to constrain neutrino mass.

ACKNOWLEDGMENTS

We are grateful to Harald Ebeling and Alex Drlica-Wagner for their contributions to this series of papers, and to Glenn Morris, Stuart Marshall and the SLAC unix support team for technical support. We also thank Giorgio Gratta and

¹³ We note that the 7-year *WMAP* results, which were released while this work was in revision, already offer some improvement. Specifically, Komatsu et al. (2010) find $M_\nu < 0.58$ eV by combining 7-year *WMAP* data with the Riess et al. (2009) H_0 prior and the BAO results of Percival et al. (2010), a noticeable improvement over the limit $M_\nu < 0.66$ eV obtained by Sekiguchi et al. (2009) from the same auxiliary data sets combined with *WMAP5*.

Naoko Kurahashi for useful discussions. Calculations were carried out using the KIPAC XOC and Orange compute clusters at the SLAC National Accelerator Laboratory and the SLAC Unix compute farm. We acknowledge support from the National Aeronautics and Space Administration (NASA) through Chandra Award Numbers DD5-6031X, GO7-8125X and GO8-9118X, issued by the Chandra X-ray Observatory Center, which is operated by the Smithsonian Astrophysical Observatory for and on behalf of NASA under contract NAS8-03060. This work was supported in part by the U.S. Department of Energy under contract number DE-AC02-76SF00515. AM was supported by a Stanford Graduate Fellowship and an appointment to the NASA Postdoctoral Program, administered by Oak Ridge Associated Universities through a contract with NASA.

REFERENCES

- Aalseth C. E. et al., 1999, *Phys. Rev. C*, 59, 2108
 Adelman-McCarthy J. K. et al., 2007, *ApJS*, 172, 634
 Aguilar A. et al., 2001, *Phys. Rev. D*, 64, 112007
 Aguilar-Arevalo A. A. et al., 2009a, *Phys. Rev. Lett.*, 102, 101802
 Aguilar-Arevalo A. A. et al., 2009b, *Phys. Rev. Lett.*, 103, 111801
 Aharmim B. et al., 2005, *Phys. Rev. C*, 72, 055502
 Ahmad Q. R. et al., 2002, *Phys. Rev. Lett.*, 89, 011301
 Ahn M. H. et al., 2006, *Phys. Rev. D*, 74, 072003
 Ahn M. H. et al., 2003, *Phys. Rev. Lett.*, 90, 041801
 Allen S. W., Rapetti D. A., Schmidt R. W., Ebeling H., Morris R. G., Fabian A. C., 2008, *MNRAS*, 383, 879
 Allen S. W., Schmidt R. W., Bridle S. L., 2003, *MNRAS*, 346, 593
 Allen S. W., Schmidt R. W., Ebeling H., Fabian A. C., van Speybroeck L., 2004, *MNRAS*, 353, 457
 Amsler C. et al., 2008, *Phys. Lett. B*, 667, 1
 Arnaboldi C. et al., 2005, *Phys. Rev. Lett.*, 95, 142501
 Arnold R. et al., 2005, *Phys. Rev. Lett.*, 95, 182302
 Bashinsky S., Seljak U., 2004, *Phys. Rev. D*, 69, 083002
 Benjamin J. et al., 2007, *MNRAS*, 381, 702
 Böhringer H. et al., 2004, *A&A*, 425, 367
 Bonamente M., Joy M. K., LaRoque S. J., Carlstrom J. E., Reese E. D., Dawson K. S., 2006, *ApJ*, 647, 25
 Bond J. R., Efstathiou G., Silk J., 1980, *Phys. Rev. Lett.*, 45, 1980
 Bradač M. et al., 2008, *ApJ*, 681, 187
 Chiang H. C. et al., 2009, arXiv:0906.1181
 Coe D., Moustakas L. A., 2009, *ApJ*, 706, 45
 Colless M. et al., 2001, *MNRAS*, 328, 1039
 Colless M. et al., 2003, arXiv:astro-ph/0306581
 Colombo L. P. L., Pierpaoli E., Pritchard J. R., 2009, *MNRAS*, 398, 1621
 Crotty P., Lesgourgues J., Pastor S., 2004, *Phys. Rev. D*, 69, 123007
 de Putter R., Zahn O., Linder E. V., 2009, *Phys. Rev. D*, 79, 065033
 Dobke B. M., King L. J., Fassnacht C. D., Auger M. W., 2009, *MNRAS*, 397, 311
 Dunkley J. et al., 2009, *ApJS*, 180, 306
 Ebeling H., Edge A. C., Böhringer H., Allen S. W., Crawford C. S., Fabian A. C., Voges W., Huchra J. P., 1998, *MNRAS*, 301, 881
 Ebeling H., Edge A. C., Henry J. P., 2001, *ApJ*, 553, 668
 Eguchi K. et al., 2003, *Phys. Rev. Lett.*, 90, 021802
 Faltenbacher A., Kravtsov A. V., Nagai D., Gottlöber S., 2005, *MNRAS*, 358, 139
 Fowler J. W. et al., 2010, arXiv:1001.2934
 Freedman W., 2009, in *American Astronomical Society Meeting Abstracts*, Vol. 214
 Fu L. et al., 2008, *A&A*, 479, 9
 Fukuda S. et al., 2002, *Phys. Lett. B*, 539, 179
 Fukuda Y. et al., 1998, *Phys. Rev. Lett.*, 81, 1562
 Fukugita M., Liu G., Sugiyama N., 2000, *Phys. Rev. Lett.*, 84, 1082
 Giacomelli G., Margiotta A., 2004, *Phys. Atom. Nucl.*, 67, 1139
 Henry J. P., Evrard A. E., Hoekstra H., Babul A., Mahdavi A., 2009, *ApJ*, 691, 1307
 Hill R. S. et al., 2009, *ApJS*, 180, 246
 Hinshaw G. et al., 2009, *ApJS*, 180, 225
 Ichikawa K., Fukugita M., Kawasaki M., 2005, *Phys. Rev. D*, 71, 043001
 Kaplinghat M., Knox L., Song Y., 2003, *Physical Review Letters*, 91, 241301
 Klapdor-Kleingrothaus H. V. et al., 2001, *Eur. Phys. J. A*, 12, 147
 Komatsu E. et al., 2009, *ApJS*, 180, 330
 Komatsu E. et al., 2010, arXiv:1001.4538
 Kowalski M. et al., 2008, *ApJ*, 686, 749
 Kraus C. et al., 2005, *Eur. Phys. J. C*, 40, 447
 Kravtsov A. V., Vikhlinin A., Nagai D., 2006, *ApJ*, 650, 128
 Lesgourgues J., Pastor S., 2006, *Phys. Rep.*, 429, 307
 Lewis A., Bridle S., 2002, *Phys. Rev. D*, 66, 103511
 Lewis A., Challinor A., Lasenby A., 2000, *ApJ*, 538, 473
 Lobashev V. M., 2003, *Nucl. Phys. A*, 719, 153
 Lueker M. et al., 2009, arXiv:0912.4317
 Mahdavi A., Hoekstra H., Babul A., Henry J. P., 2008, *MNRAS*, 384, 1567
 Mantz A., Allen S. W., Ebeling H., Rapetti D., 2008, *MNRAS*, 387, 1179
 Mantz A., Allen S. W., Rapetti D., Ebeling H., 2009a, arXiv:0909.3098 (Paper I)
 Mantz A., Allen S. W., Ebeling H., Rapetti D., Drlica-Wagner A., 2009b, arXiv:0909.3099 (Paper II)
 Nagai D., Vikhlinin A., Kravtsov A. V., 2007, *ApJ*, 655, 98
 Newman A. B., Treu T., Ellis R. S., Sand D. J., Richard J., Marshall P. J., Capak P., Miyazaki S., 2009, *ApJ*, 706, 1078
 Nolta M. R. et al., 2009, *ApJS*, 180, 296
 Oguri M., 2007, *ApJ*, 660, 1
 Percival W. J. et al., 2007, *ApJ*, 657, 51
 Percival W. J. et al., 2010, *MNRAS*, 401, 2148
 Perotto L., Lesgourgues J., Hannestad S., Tu H., Y Y Wong Y., 2006, *Journal of Cosmology and Astro-Particle Physics*, 10, 13
 Rapetti D., Allen S. W., Mantz A., 2008, *MNRAS*, 388, 1265
 Rapetti D., Allen S. W., Mantz A., Ebeling H., 2009a, *MNRAS*, 400, 699

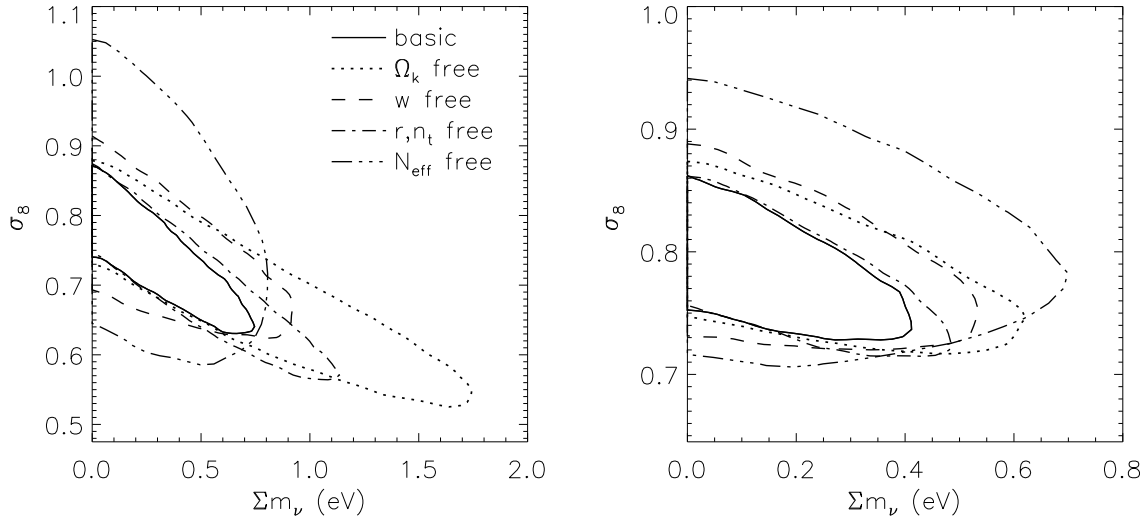


Figure 6. (Black and white version of Figure 2.) Joint 95.4 per cent confidence regions for M_ν and σ_8 for various cosmological models. Solid contours correspond to the basic Λ CDM+ M_ν model, dotted contours are marginalized over Ω_k , dashed contours over w , dot-dashed over r and n_t , and 3-dot-dashed over N_{eff} . The left panel shows constraints obtained from the combination of CMB, f_{gas} , SNIa and BAO data; the right panel shows results that include the XLF in addition to those data. No external prior on H_0 is used.

- Rapetti D., Allen S. W., Mantz A., Ebeling H., 2009b, arXiv:0911:1787
- Rapetti D., Allen S. W., Weller J., 2005, MNRAS, 360, 555
- Rasia E. et al., 2006, MNRAS, 369, 2013
- Reichardt C. L. et al., 2009, ApJ, 694, 1200
- Reid B. A., Verde L., Jimenez R., Mena O., 2009, arXiv:0910.0008
- Riess A. G. et al., 2009, ApJ, 699, 539
- Rozo E. et al., 2010, ApJ, 708, 645
- Saha P., Coles J., Macciò A. V., Williams L. L. R., 2006, ApJL, 650, L17
- Sanchez M. et al., 2003, Phys. Rev. D, 68, 113004
- Schmidt F., Vikhlinin A., Hu W., 2009, Phys. Rev. D, 80, 083505
- Schmidt R. W., Allen S. W., Fabian A. C., 2004, MNRAS, 352, 1413
- Sekiguchi T., Ichikawa K., Takahashi T., Greenhill L., 2009, arXiv:0911.0976
- Spergel D. N. et al., 2007, ApJS, 170, 377
- Tegmark M. et al., 2004, Phys. Rev. D, 69, 103501
- Terenio I., Schimd C., Uzan J.-P., Kilbinger M., Vincent F. H., Fu L., 2009, A&A, 500, 657
- Thomas S. A., Abdalla F. B., Lahav O., 2009, arXiv:0911.5291
- Trümper J., 1993, Science, 260, 1769
- Vallinotto A., Viel M., Das S., Spergel D. N., 2009, arXiv:0910.4125
- Vikhlinin A. et al., 2009, ApJ, 692, 1060
- Wang S., Haiman Z., Hu W., Khoury J., May M., 2005, Phys. Rev. Lett., 95, 011302
- Zhang Y. et al., 2010, arXiv:1001.0780

This paper has been typeset from a $\text{\TeX}/\text{\LaTeX}$ file prepared by the author.